Synthetic, Structural and Computational Studies on Heavier Tetragen and Chalcogen Triazenide Complexes.

Kerry R. Flanagan,[a] James D. Parish,[a] Mark A. Fox[b*] and Andrew L. Johnson.[a*]

[a)]Department of Chemistry, University of Bath, Claverton Down, Bath, BA2 7AY. UK.

[b)]Department of Chemistry, University of Durham, South Road, Durham, DH1 3LE. UK.

KEYWORDS : Triazenide, Germanium, Tin, Lead, Selenium, Tellurium, DFT.

Supporting Information Placeholder

ABSTRACT: The syntheses of the triazenide complexes [{N(N^{Dipp})$_2$}$_2$M] (Dipp = 2,6-*di-iso*propylphenyl; M = Ge(II) (**1**), Sn(II) (**2**), Pb(II) (**3**) and Te(II) (**5**)) are described for the first time. These compounds have been characterized by single-crystal X-ray diffraction and heteronuclear NMR spectroscopy. DFT calculations were employed to confirm the presence and nature of the stereochemically active lone pairs in **1**-**5**, alongside the Gibbs energy changes for their general synthesis, which enable the rationalisation of observed reactivities.

Amidinates, guanidinates and triazenides[1, 2] are part of the wider family of monoanionic-heteroallylic ligands,[3-7] and are extremely common ligands in co-ordination chemistry (Chart 1). In main group chemistry, they are often used to kinetically stabilize coordinatively unsaturated and typically low-oxidation state complexes.[8-22] The attraction of these monoanionic, κ^2-N,N coordinating systems is due to their relative ease of synthesis[13, 23] and their variability with respect to steric and electronic properties. For heteroallylic ligands, such properties may be fine-tuned by the informed choice of substituents on either the terminal nitrogen atoms or the central hetero-atom (Chart 1). As such, these versatile ligands have been employed in complexes across the transition metals,[24-29] lanthanide and actinide elements,[15, 30-33] as well as a limited number of p-block metals.[18-22, 34, 35]

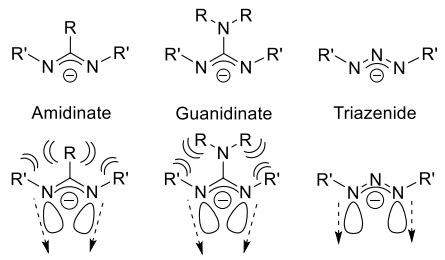

Chart 1: General form of the amidinate, guanidinate and triazenide anions and the effect of sterics on *N*-orbital projection.

Triazenides, in contrast to amidinates and guanidinates which are comparable in their bonding modes, have not been as popular as ligands for the main group elements, despite the fact that simple triazenes have been known and used as ligands for many years. In contrast, these ligands have been popular for transition metals, and just as with their amidinate and guanidinate congeners, triazenide ligands display a range of monodentate and chelating coordination arrangements (Chart 2).[1] The differences in electronegativity of the central element of the ligands (N vs C)[12] affects the electron donating ability of the terminal [19] groups, as well as the relative projection of the orbitals on the two terminal [19] donor groups. In triazenide systems these orbitals are approximately parallel due to the lack of steric perturbation caused by substituent groups on the central N-atom, resulting in wider bite angles compared to the related amidinate and guanidinate systems. The presence of a central nitrogen atom in the triazene pro-ligands also increases the acidity of the pro-ligands[36] relative to those of amidine and guanidine counterparts. Accordingly, triazenide ligands are generally considered to be more weakly coordinated to metals, with amplified electrophilicity at the bound metal atom.[36] Collectively these features have promoted further interest in the chemistry of triazenide ligands of the main group elements. More recently, a remarkable series of P(I), As(I) and Sb(I) complexes have been reported using triazenide ligands.[37]

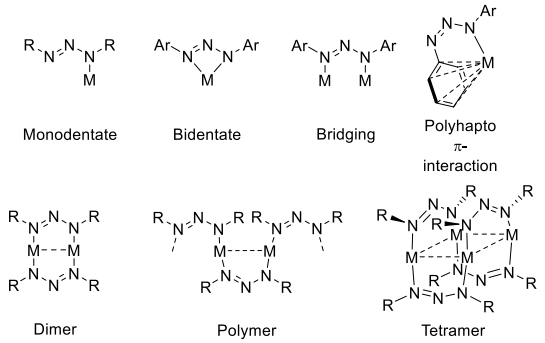

Chart 2: Generic bonding modes and typical structures of triazenide complexes.

Recent interest in metal triazenide complexes, especially those of group 1, group 2, zinc and group 13 metals, has in part been due to their extensive coordination chemistry, but has also, in selected cases, been due to their potential suitability in chemical vapor deposition (CVD) and sol gel processes for the production of metal nitrides.[26, 27] Surprisingly, triazenide complexes of the group 14 and 15 elements have hitherto been limited to the silyltriazene complex [{^{t}Bu$_3$Si-N=N-N(SnMe$_3$)Si^{t}Bu$_3$}], formed from the reaction of [{^{t}Bu$_3$Si-N$_3$-Si^{t}Bu$_3$}]Na with Me$_3$SnCl reported by Veith[38] and the lead triazenide {(Me$_3$Si)$_3$SiN$_3$Ad}PbSi(SiMe$_3$)$_3$ (Ad = adamantyl), formed from the reaction of AdN$_3$ with {(Me$_3$Si)$_3$Si}$_2$Pb by Klinkhammer.[39] In this report, we present for the first time the synthesis and molecular structures of the M(II) triazenide complexes [{L$^{(Dipp)}$}$_2$M] (L$^{(Dipp)}$ =

N(NDipp)$_2$, Dipp = 2,6-*di*-*iso*propylphenyl; M = Ge(II), Sn(II), Pb(II) and Te(II)).

Results and Discussion

The divalent complexes [{L$^{(Dipp)}$}$_2$M], M = Ge(II) (**1**), Sn(II) (**2**) and Pb(II) (**3**) were all synthesized by deprotonation of two equivalents of the triazene [(Dipp)N=N-N(H)(Dipp)], H{L$^{(Dipp)}$}, with the corresponding *bis*-amides [M{N(SiMe$_3$)$_2$}$_2$] (M = Ge, Sn and Pb) in toluene (eq. 1). All three compounds showed a high degree of solubility in toluene and hexane.

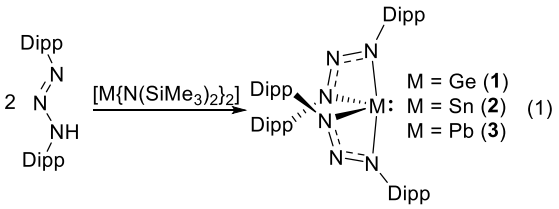

(1)

Subsequent recrystallization of the products from hexanes and storage at low temperature (-28 °C) resulted in the formation of crystalline materials suitable for single crystal X-ray diffraction. In all cases the products were characterized by solution state NMR (^{1}H, ^{13}C, ^{119}Sn) spectroscopy and elemental analysis.

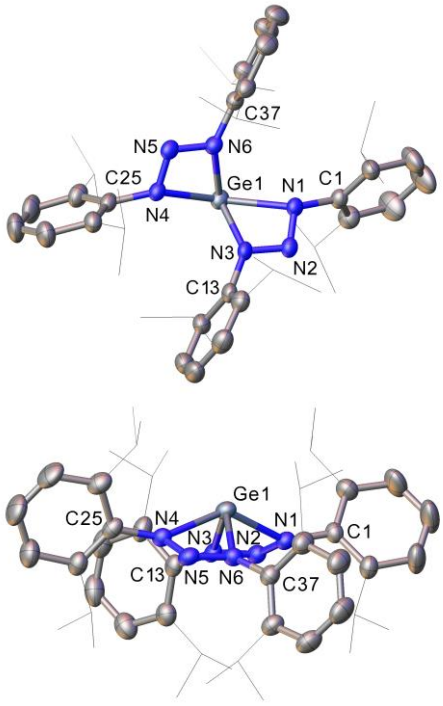

Figure 1. Two views of the molecule [{L$^{(Dipp)}$}$_2$Ge] (**1**) are shown, with thermal ellipsoids drawn at the 50% probability level. The {^{i}Pr} groups are shown as wire frames and hydrogen atoms are omitted for clarity. Similar experimental geometries for [{L$^{(Dipp)}$}$_2$Sn] (**2**) and [{L$^{(Dipp)}$}$_2$Pb] (**3**) are depicted in Figure S1. Selected bond lengths [Å], angles, and torsion angles [°] in sequence Ge (**1**), Sn (**2**), Pb (**3**): M1–N1 2.186(2), 2.3402(16), 2.431(2); M1–N4 2.206(2), 2.3380(16), 2.434(2); M1–N3 2.014(2), 2.2289(17), 2.332(3); M1–N6 2.002(2), 2.2162(16), 2.363(2); N1–M1–N4 137.37(7), 129.18(6), 125.51(8); N3–M1–N6 104.17(8), 101.40(6), 100.46(9); N1–M1–N3 59.48(7), 55.16(6), 53.02(9); N4–M1–N6 59.73(7), 55.44(6), 52.59(8).

The ^{1}H NMR spectroscopic data of **1** and **2** (see Supporting Information), recorded in [D$_6$]-benzene solutions at room temperature, were consistent with simple symmetrical structures in which the methyl groups in 2,6-*di*-*iso*propylphenyl moieties are magnetically inequivalent. For **1**, two doublets at δ = 1.12 and 1.10 ppm are observed, alongside a broad multiplet at δ = 3.41 ppm and resonances for the aromatic region δ = 7.06-7.13 ppm in the ^{1}H NMR spectrum. This is consistent with restricted rotations about the nitrogen-phenyl bonds such that the methyl groups on either side of the plane of the phenyl ring are in different magnetic environments. The Sn(II) complex (**2**) NMR spectroscopy (^{1}H and ^{13}C) reveals a similar series of resonances and the ^{119}Sn chemical shift was observed at δ = -198.9 ppm.

For the Pb(II) complex (**3**), the ^{1}H NMR spectrum shows the presence of one doublet and one septet, at δ = 1.12 and 3.40 ppm respectively, consistent with free rotation about the nitrogen-phenyl bonds on the NMR time scale thus rendering all methyl groups in the {Dipp} groups magnetically equivalent. The ^{207}Pb{^{1}H} NMR spectrum showed a single broad resonance at δ = 2520 ppm, which correlates well with the predicted ^{207}Pb chemical shifts (~ δ = 2893 ppm) using Wrackmeyer's correlation concerning the corresponding tin analog.[40]

The molecular structure of **1** is shown in Figure 1, along with significant bond distances and angles, for all three isostructural complexes. The molecular structures of the analogous complexes [{L(^{Dipp})}$_2$M] (M = Sn (**2**) and M = Pb (**3**) are included in the supplementary information. The compounds crystallize in the monoclinic space groups P2$_{1/n}$ (**1**) and P2$_{1/c}$ (**2** and **3**) respectively, and are essentially isostructural with the known formamidinate systems [{HC(N^{Dipp})$_2$}$_2$M] (M = Ge,[41] Sn[42] and Pb[43]).

Average Bond Lengths (Å)

		Ge		Sn		Pb	
	E	N	C(H)	N	C(H)	N	C(H)
	a	2.195	2.276	2.339	2.375	2.43	2.46
	b	2.008	2.001	2.223	2.232	2.35	2.35
	c	1.31	1.31	1.31	1.31	1.30	1.30
	Ref:	This work	41	This work	42	This work	43

Average Bond Angles (°)

		Ge		Sn		Pb	
	E	N	C(H)	N	C(H)	N	C(H)
	α	59.6	62.0	55.3	57.9	52.8	55.3
	β	106.7	115.0	108.4	116.7	109.5	118.1
	θ	137.3	140.6	129.2	133.2	125.5	129.6
	ϕ	104.2	102.8	101.4	102.4	100.5	100.1
	Ref:	This work	41	This work	42	This work	43

Figure 2. A comparison of average bond lengths and bond angles for the isostructural triazenide complexes, **1**-**3**, and the related formamidinate complexes [{HC(N^{Dipp})$_2$}$_2$M] (M = Ge,[41] Sn[42] and Pb[43]).

All three isostructural complexes (**1**-**3)** possess four coordinate metal centers supported by two bidentate κ^2-triazenide ligands and are structurally comparable to the previously reported formamidinate complexes of the form [{HC(N^{Dipp})$_2$}$_2$M] (M = Ge,[41] Sn[42] and Pb[43]). While the M-N bonds in **1**-**3** are asymmetric, with one ca. 0.1 Å longer, the bond lengths increase as expected in the order Ge < Sn < Pb, and are in good agreement with the interatomic distances reported for comparable germanium, tin and lead complexes.[43-46] While the asymmetric M-N bonds may be suggestive of some M–N(amido) vs. M–N(amino) type binding, this is not reflected in the N–N bond lengths of the triazenides, where the N–N bond lengths are statistically similar in each compound.

As can be seen from Figure 2, a comparison between complexes **1**-**3** and the known formamidinate complexes [{HC(N^{Dipp})$_2$}$_2$M] (M = Ge,[41] Sn[42] and Pb[43]), general trends within this family of complexes can be observed. For a given metal (e.g. Ge), the equatorial M-N interactions (**b**) for the triazenide and formamidinate ligands are very similar [2.008 vs 2.001 Å]. The differences between complexes arise in the axial M-N interactions (**a**) [2.195 vs 2.276 Å] which is in turn a result of the more acute angle at the central atom (i.e. N or C(H)) of the heteroallylic ligand. The smaller N atom induces a more acute N-E-N angle [106.7° vs 115.0°].

Across complexes **1**-**3** the two triazenide ligands are orientated in a cisoidal fashion about the metal centres, which leaves a significant area of the coordination sphere of the metal atom exposed which is indicative of a stereochemically active lone pair on the metal centres. Due to their acute bite angles [N1-M1-N3 and N4-M1-N6 (see Fig. 1)], which gradually reduce in the sequence Ge > Sn > Pb, the four nitrogen atoms are disposed such that the geometries about the central metal atom lie somewhere between trigonal bipyramidal and square-based pyramidal geometries, as determined by the geometric value τ [τ_{Ge} = 0.55; τ_{Sn} = 0.46; τ_{Pb} = 0.42]. where the geometry about the metal centre lies closest to trigonal bipyramidal for compound **1**. The geometric sequence **1** < **2** < **3** is apparently a result of the increasing size, diffuseness and s-character of the lone pair on the metals (vide infra).[47] As with the related formamidinate[41-43] and guanidinate[46] systems which contain the sterically demanding {Dipp} groups[23, 48-50] Ref Chlupaty, Cole, Green, Nimitsiriwat the aromatic rings are twisted out of the plane of the cyclic {MN$_3$} cores, with angles approaching perpendicularity (Table S2).

Initial attempts to prepare the heteroleptic triazenide/amide complexes [{L$^{(Dipp)}$}M{N(SiMe$_3$)$_2$}] by direct stoichiometric (1:1) reaction of *bis*-amides [M{N(SiMe$_3$)$_2$}$_2$] (M = Ge, Sn and Pb) with H{L$^{(Dipp)}$} in both toluene and THF were unsuccessful, resulting in the isolation of the *bis*(triazenide) compounds **1**-**3**. We attribute this failure to prepare the heteroleptic-M(II) species to the stronger acidity of the triazenide ligands {N-H} relative to that of the H-N(SiMe$_3$)$_2$.

The reactivity of the bulky triazene H{L$^{(Dipp)}$} with chalcogen analogues [Se{N(SiMe$_3$)$_2$}$_2$] and [Te{N(SiMe$_3$)$_2$}$_2$] in toluene was also investigated. In both cases, attempts were made to synthesize and isolate the homoleptic and heteroleptic species [{L$^{(Dipp)}$}M(II){N(SiMe$_3$)$_2$}] (M = Se and Te) and [{L$^{(Dipp)}$}$_2$Se] (**4**) and [{L$^{(Dipp)}$}$_2$Te] (**5**) using the same protocols as described earlier for the tetragens. In the case of the selenium compounds, no reaction was observable, irrespective of stoichiometry of triazene used, with the starting materials [Se{N(SiMe$_3$)$_2$}$_2$] and H{L$^{(Dipp)}$} being isolated on several occasions from the reaction mixtures, indicative of a lack of reactivity, rather than instability of a product. Despite repeated attempts to form the analogous Se(II) systems, including an investigation into the reactivity of Se_2Cl_2 with the lithiated triazenide ligand, [Li{L$^{(Dipp)}$}], made *in-situ* from reaction of H{L$^{(Dipp)}$} with [Li{N(SiMe$_3$)$_2$}], the desired complex [{L$^{(Dipp)}$}$_2$Se] remains elusive.

By contrast, in the case of tellurium, the expected *bis*-triazenide complex [{L$^{(Dipp)}$}$_2$Te] (**5**) was formed and isolated from concentrated toluene solution at −28 °C (eq. 2). The ^{1}H NMR spectroscopic data for **5** (see Supporting Information), recorded in [D$_6$]-benzene solutions at room temperature, are consistent with a simple symmetrical structure in which the methyl groups of the {Dipp} moieties are equivalent. One broad doublet at δ = 1.21 ppm, a single broad septet at δ = 3.47 ppm and resonances for the aromatic region δ = 7.07-7.22 ppm are observed in the ^{1}H NMR spectrum.

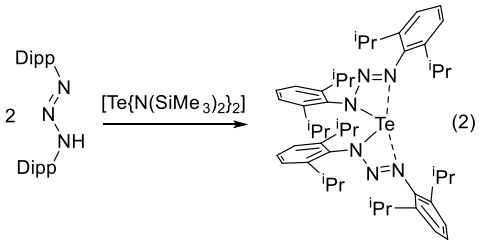

(2)

5

The molecular structure of **5** is shown in Figure 3 along with significant bond distances and angles. The compound crystallized in the triclinic space group P-1. Here, the central Te atom is four coordinate with the two {L$^{(Dipp)}$} ligands, which act as bidentate chelating ligands to the Te centre, arranged such that the Te and the six nitrogen atoms of the {L$^{(Dipp)}$} ligands are approximately coplanar (an angle of 19.16° exists between the two {TeN$_3$} rings fused at Te). This results in a distorted square planar geometry or a trapezoidal-planar configuration. The sum of the angles around Te is 361.5(1)°. The overall geometry about the Te atom is suggestive of the presence of two stereoactive lone pairs of electrons on Te centre, which lie above and below this {TeN$_4$} plane (*ibid*).

Despite the κ^2-like coordination of the triazenide ligands, the two short Te-N bonds [Te1-N3 2.1698(12) Å; Te1-N4 2.1608(12) Å] are slightly longer than other Te(II)-N single bonds observed in structurally characterized tellurium(II) *bis*-amide complexes, such as [Te{N(SiMe$_3$)$_2$}][51] and [Te{NMe$_2$}$_2$]$_\infty$ [52] [Te-N Ave. 2.05 Å]. This bond lengthening may be a result of steric repulsion between the coplanar {Dipp} moieties. Contrastingly, the longer Te-N interactions [Te1-N1 2.3996(12)Å; Te1-N6 2.6242(12) Å], although shorter than the sum of the van der Waals radii of Te and N (3.70 Å), are most aptly described as weakly co-ordinating Te···N interactions, similar to those observed in polymeric [Te{NMe$_2$}$_2$]$_\infty$ [average intermolecular Te···N distance 2.96 Å].[52]

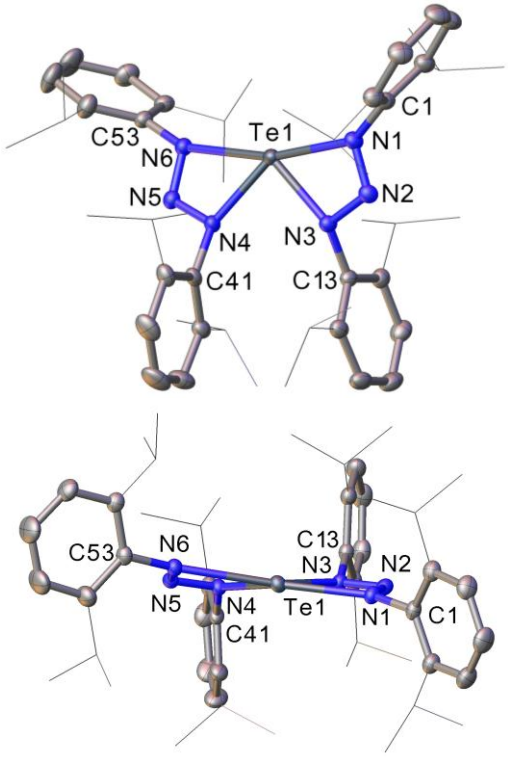

Figure 3. Two views of the molecule structure of the complex [{L(Dipp)}$_2$Te] (**5**), with thermal ellipsoids drawn at the 50% probability level. The {^{i}Pr} groups are shown as wire frames and hydrogen atoms have been omitted for clarity. Selected bond lengths [Å], angles, and torsion angles [°]: Te1–N1 2.3996(12); Te1–N3 2.1698(12); Te1–N4 2.1608(12); Te1–N6 2.6242(12); N1-N2 1.2789(17); N2-N3 1.3290(17); N4-N5 1.3309(17); N5-N6 1.2771(17); N1–Te1–N6 165.50(4); N3–Te1–N4 88.59(4); N1–Te1–N3 54.92(4); N4–Te1–N6 52.41(4).

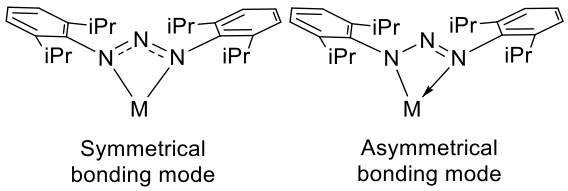

Chart 3: Symmetric and asymmetric metal-triazenide bonding motifs.

The asymmetric Te-N bonding is mirrored in the N-N distances of the {L$^{(Dipp)}$} ligands which, when compared to complexes **1**-**3**, display localized bonding with one single N-N bond [N3-N2 1.3290(17) Å; N4-N5 1.3309(17) Å] and one N=N [N1-N2 1.2789(17) Å; N5-N6 1.2771(17) Å] bond (Chart 3) and results in ligand bite angles of 67.81(9)° [N1-Te-N3] and 68.4(2)° [N4-Te-N6]. A N3-Te-N4 bond angle of 88.6° for the shorter Te-N bonds suggests the absence of *sp*-hybridisation at the Te(II) centre and that the tellurium–ligand bonds almost exclusively involve the *p*-orbitals; the nature of the electron lone pairs in compound **5** may therefore be considered as populating a $5s^2\,5p^2$ configuration. As with complexes **1**-**3**, the sterically demanding 2,6-*di*-*iso*-propylphenyl rings on **5** are twisted out of the plane of the cyclic {MN$_3$} cores, with angles between the Te1-N1-N2-N3 and Te-N4-N5-N6 planes and the phenyl rings {C1-C6} and {C13-C18} / {C41-C46} and {C53-C58} respectively approaching perpendicular [{TeN$_3$}-{C1-C6}: 78.72(3)°, [{TeN$_3$}-{C13-C18}: 85.83(3)°, [{TeN$_3$}-{C41-C46}: 78.61(3)°, [{TeN$_3$}-{C53-C58}: 72.18(3)°.

Attempts to synthesize and isolate the heteroleptic triazenide/amide complex, [{L$^{(Dipp)}$}Te{N(SiMe$_3$)$_2$}], by direct stoichiometric (1:1) reaction of [Te{N(SiMe$_3$)$_2$}$_2$] with H{L$^{(Dipp)}$} in a range of solvents were unsuccessful resulting in the isolation of the heteroleptic *bis*-triazenide complex **5**.

Computational studies

To support our interpretations of the experimental geometries and observed NMR data for **1**, **2** and **5,** and to examine whether compound **4** could be successfully synthesized, hybrid density functional theory (DFT) calculations were undertaken. The optimized geometries for **1**, **2** and **5** are in accord with the experimental geometries (Table S3) where electronic structure calculations confirm the presence of one stereochemically active lone pair per central atom in **1** and **2** and two stereochemically active lone pairs at Te in **5**.

Figure 4 shows the highest occupied molecular orbital (HOMO) for **1** where the lone pair is predominantly located. The percentages of s and p character are not obtained directly from the electronic structure calculations so the s and p contributions here are quoted from NBO analyses. Generally, NBO analyses on optimized geometries make correct predictions about the number of lone pairs and the percentage participation of s and p orbitals in making up a particular lone pair thus matching hybridization concepts. However, these analyses show the occupancies in localized MOs instead of the expected geometrical location of the lone pairs as observed from the relevant highest occupied MOs from electronic structure calculations.[53] NBO analyses reveal that the lone pair contains 70% s-character for Ge in **1** and 84% s-character for Sn in **2** supporting the increasing structural distortion from **1** to **2**.

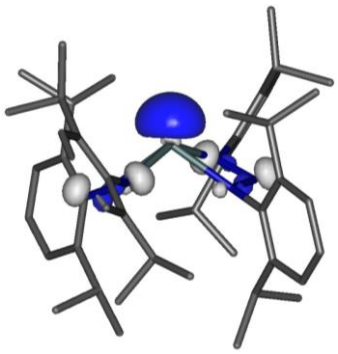

Figure 4. A representation of the HOMO of **1** showing the lone pair on the metal.

The highest occupied molecular orbitals, HOMO and HOMO-1 for **5** corresponding to the lone pairs are shown in Fig. 5. The lone pairs at Te in **5** are populated with $5s^2$ and $5p^2$ orbital electrons according to NBO computations. One lone pair at Te has 93% s- and 7% p-character and the other lone pair has 100% p-character.

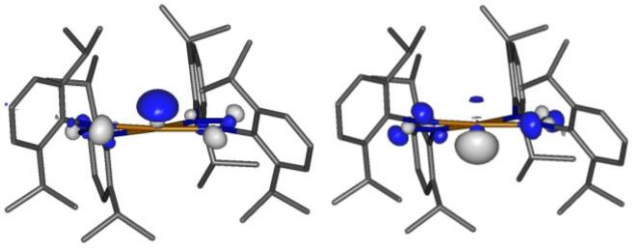

Figure 5. A representation of the HOMO and HOMO-1 orbitals of **5,** depicting the two stereoactive lone pairs on Te.

The non-equivalent NMR peaks assigned to the methyl groups of **1** and **2** suggest that the energies required for inversion at the metal atom are too high for fluxional inversion processes in solutions to render equivalent methyl groups. The energies for the transition state geometries involved in the fluxional inversion processes were estimated to be 34.1 kcal mol^{-1} higher than the energy minimum for **1** and 43.9 kcal mol^{-1} higher than the energy minimum for **2.** Both Gibbs energy barriers calculated at 298.15 K are indeed too high for the fluxional inversion processes to take place in solutions at ambient temperatures. However, the Gibbs energy of the corresponding transition state geometry involved in the fluxional process for **5** is only 13.4 kcal mol^{-1} higher in energy than the energy minimum. Such fluxional processes are expected in solutions of **5** thus peaks assigned to equivalent methyl groups are observed experimentally. These transition state geometries are visualized in Figures S3-S8.

A geometry optimization of the unknown Se compound, **4**, was carried out using the geometry of **5**, determined by single crystal X-ray diffraction, as the starting geometry with Te replaced by Se. One of the four {Dipp} groups changed orientation (from 66° to 22°) during the optimization process to give a minimum. It seems that there is a significant steric effect on the Dipp group orientations by replacing the Te atom with the smaller Se atom (Figure 6). The calculated Gibbs energy changes for the general reaction:

$$2\ \{L^{(Dipp)}\}H + [M\{N(SiMe_3)_2\}] \rightarrow [\{L^{(Dipp)}\}_2\ M] + 2\ (Me_3Si)_2NH$$

were -34.0, -43.6, -7.9 and -23.2 kcal mol^{-1} for **1**, **2**, **4** and **5** respectively (Table S4)**.** These relative values show **4** to be less favorable thermodynamically than the others but do not rule out the possibility that **4** could be made experimentally.

Conclusions

The purpose of this study was to generate a new class of main group triazenide complexes. As a key part of the study, we also wished to explore the nature of the bonding in an isostructural series of germanium, tin and lead complexes, as well as the related selenium and tellurium complexes, to gain an appreciation of the nature and relative influences of the lone pairs.

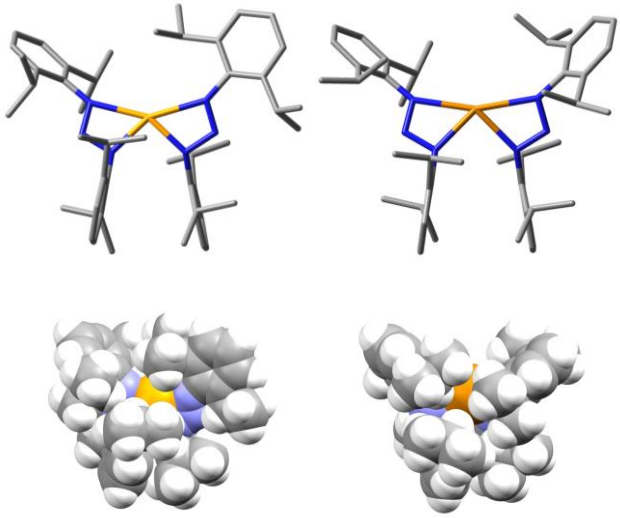

Figure 6. Optimized geometries for **4** (left) and **5** showing the twisted {Dipp} group orientation in **4** due to steric effects by the smaller Se atom in **4**.

To this end, we have generated the first reported examples of Ge(II), Sn(II), Pb(II) and Te(II) bistriazenide complexes. The tetragen (Ge, Sn, Pb) systems all appear to be relatively stable. The solid state molecular structures of these complexes showed that the geometry around the metal center changes from trigonal bipyramidal to square-based pyramidal as the group is descended from Ge to Sn and Pb. By contrast, attempts to synthesize the chalcogen complexes $[\{L^{(Dipp)}\}_2M]$ (M = Se, Te) were met with mixed success. Multiple attempts to make the Se derivative were unsuccessful, whereas the Te-triazenide compound was formed in near quantitative yield. The solid state structure of the latter reveals a distorted square planar geometry about the central four-coordinate Te atom.

Electronic structure calculations confirm the presence of one stereochemically active lone pair per central atom in the tetragon complexes and two stereochemically active lone pairs in the tellurium complex. Hybrid-DFT calculations also suggest that the Gibbs free energy barriers to metal inversion are too high to allow fluxionality to take place in solution for the Ge and Sn complexes. In the case of the Te complex, the Gibbs free energy of the fluxional process is only 13.4 kcal mol^{-1} higher in energy than the calculated energy minimum, consistent with the observation that the dynamic behavior occurs in solution on the NMR timescale. Energies from geometry optimizations of the unknown Se triazenide complex along with other complexes synthesized, show that the formation of the Se molecule is the least thermodynamically viable. Synthesis of a selenium-triazenide complex may prove possible using a triazenide ligands with reduced steric bulk, and will be investigated in the near future.

Supporting Information

The Supporting Information is available free of charge on the ACS Publications website at DOI:

Details of experimental methods and materials; FTIR, EPR, XAS, and XRD data collection details (PDF)

Accession Codes

CCDC 1953499 to 1953502 for complexes **1**-**3** and **5**, respectively contain the supplementary crystallographic data for this paper. These data can be obtained free of charge via www.ccdc.cam.ac.uk/data_request/cif, or by contacting The Cambridge Crystallographic Data Centre, 12 Union Road, Cambridge CB2 1EZ, UK; fax: + 44 1223 336033.

AUTHOR INFORMATION

Corresponding Author

*E-mail: A.L.Johnson@bath.ac.uk (A. L. Johnson).
*E-mail: M.A.Fox@dur.ac.uk (M. A. Fox).

Author Contributions

The manuscript was written through contributions of all authors. / All authors have given approval to the final version of the manuscript.

Funding Sources

This work was funded by the University of Bath, in the form of University PhD Studentships to KRF and JDP.

REFERENCES

(1) Moore, D. S.; Robinson, S. D. In *Advances in Inorganic Chemistry*; **1986,** 1-68.

(2) Vrieze, K.; van Koten, G. In *Comprehensive Coordination Chemistry*; Pergamon: Oxford, 1987; Vol. 2, 189-244. .

(3) Edelmann, F. T. In *Advances in Organometallic Chemistry*; Academic Press: 2008; Vol. 57, 83-352.

(4) Edelmann, F. T. Lanthanide Amidinates and Guanidinates: From Laboratory Curiosities to Efficient Homogeneous Catalysts and Precursors for Rare-Earth Oxide Thin Films. *Chem. Soc. Rev.* **2009,** 38, 2253-2268.

(5) Jones, C. Bulky Guanidinates for the Stabilization of Low Oxidation State Metallacycles. *Coord. Chem. Rev.* **2010,** 254, 1273-1289.

(6) Barry, S. T. Amidinates, Guanidinates and Iminopyrrolidinates: Understanding Precursor Thermolysis to Design a Better Ligand. *Coord. Chem. Rev.* **2013,** 257, 3192-3201.

(7) Chlupatý, T.; Růžička, A. Hybrid Amidinates and Guanidinates of Main Group Metals. *Coord. Chem. Rev.* **2016,** 314, 103-113.

(8) Lee, H. S.; Niemeyer, M. Inverse Aggregation Behavior of Alkali-Metal Triazenides. *Inorg. Chem.* **2006,** 45, 6126-6128.

(9) Gyton, M. R.; Bhadbhade, M.; Cole, M. L. A Flexible, Extremely Sterically Demanding Triazenide Ligand: Synthesis and Coordination Chemistry. *Z. Anorg. Allg. Chem.* **2019,** 645, 768-776.

(10) McKay, A. I.; Cole, M. L. Structural Diversity in a Homologous Series of Donor Free Alkali Metal Complexes Bearing a Sterically Demanding Triazenide. *Dalton Trans.* **2019,** 48, 2948-2952.

(11) Westhusin, S.; Gantzel, P.; Walsh, P. J. Synthesis and Crystal Structures of Magnesium and Calcium Triazenide Complexes. *Inorg. Chem.* **1998,** 37, 5956-5959.

(12) Hauber, S.-O.; Lissner, F.; Deacon, G. B.; Niemeyer, M. Stabilization of Aryl-Calcium, -Strontium, and -Barium Compounds by Designed Steric and π-Bonding Encapsulation. *Angew. Chem. Int. Ed.* **2005,** 44, 5871-5875.

(13) Barrett, A. G. M.; Crimmin, M. R.; Hill, M. S.; Hitchcock, P. B.; Kociok-Köhn, G.; Procopiou, P. A. Triazenide Complexes of the Heavier Alkaline Earths: Synthesis, Characterization, And Suitability for Hydroamination Catalysis. *Inorg. Chem.* **2008,** 47, 7366-7376.

(14) Barrett, A. G. M.; Crimmin, M. R.; Hill, M. S.; Hitchcock, P. B.; Lomas, S. L.; Procopiou, P. A.; Suntharalingam, K. Catalytic 2,3,4-Hexatriene Formation by Terminal Alkyne Coupling at Calcium. *Chem. Commun.* **2009,** 2299-2301.

(15) Lee, H. S.; Niemeyer, M. Homoleptic Heavy Alkaline Earth and Europium Triazenides. *Inorg. Chem.* **2010,** 49, 730-735.

(16) Kalden, D.; Krieck, S.; Görls, H.; Westerhausen, M. 1,3-Bis(2,4,6-trimethylphenyl)Triazenides of Potassium, Magnesium, Calcium, and Strontium. *Dalton Trans.* **2015,** 44, 8089-8099.

(17) Kalden, D.; Krieck, S.; Görls, H.; Westerhausen, M. Coordination Chemistry of N-(2-Pyridylethyl)-Substituted Bulky Amidinates and Triazenides of Magnesium. *Eur. J. Inorg. Chem.* **2018,** 4361-4369.

(18) Leman, J. T.; Braddock-Wilking, J.; Coolong, A. J.; Barron, A. R. 1,3-Diaryltriazenido Compounds of Aluminum. *Inorg. Chem.* **1993,** 32, 4324-4336.

(19) Leman, J. T.; Roman, H. A.; Barron, A. R. Five- and Six-Coordinate Organometallic Compounds of Indium. *Organometallics* **1993,** 12, 2986-2990.

(20) Uhl, W.; El-Hamdan, A.; Lawerenz, A. Investigations into the Reactivity of Organoelement Gallium and Indium Subhalides - Syntheses of Digallium and Diindium Acetylacetonates. *Eur. J. Inorg. Chem.* **2005,** 1056-1062.

(21) Lee, H. S.; Hauber, S.-O.; Vinduš, D.; Niemeyer, M. Isostructural Potassium and Thallium Salts of Sterically Crowded Triazenes: A Structural and Computational Study. *Inorg. Chem.* **2008,** 47, 4401-4412.

(22) Alexander, S. G.; Cole, M. L.; Forsyth, C. M.; Furfari, S. K.; Konstas, K. Bulky Triazenide Complexes of Alumino- and Gallohydrides. *Dalton Trans.* **2009,** 2326-2336.

(23) Nimitsiriwat, N.; Gibson, V. C.; Marshall, E. L.; Takolpuckdee, P.; Tomov, A. K.; White, A. J. P.; Williams, D. J.; Elsegood, M. R. J.; Dale, S. H. Mono- versus Bis-chelate Formation in Triazenide and Amidinate Complexes of Magnesium and Zinc. *Inorg. Chem.* **2007,** 46, 9988-9997.

(24) Zarkesh, R. A.; Heyduk, A. F. Reactivity of Organometallic Tantalum Complexes Containing a Bis(phenoxy)amide $(ONO)^{3-}$ Ligand with Aryl Azides and 1,2-Diphenylhydrazine. *Organometallics* **2011,** 30, 4890-4898.

(25) Tejel, C.; Ciriano, M. A.; Sola, E.; del Río, M. P.; Ríos-Moreno, G.; Lahoz, F. J.; Oro, L. A. Dimetallic Dioxygen Activation Leading to a Doubly Oxygen-Bridged Dirhodium Complex. *Angew. Chem. Int. Ed.* **2005,** 44, 3267-3271.

(26) Soussi, K.; Mishra, S.; Jeanneau, E.; Millet, J.-M. M.; Daniele, S. Asymmetrically Substituted Triazenes as Poor Electron Donor Ligands in the Precursor Chemistry of Iron(II) for Iron-Based Metallic and Intermetallic Nanocrystals. *Dalton Trans* **2017,** 46 (38), 13055-13064.

(27) Soussi, K.; Mishra, S.; Jeanneau, E.; Mantoux, A.; Daniele, S. Synthesis, Characterization and Thermal Transport Properties of Heteroleptic N-alkyl Triazenide Complexes of Titanium(IV) and Niobium(V). *Polyhedron.* **2018,** 152, 84-89.

(28) Litlabø, R.; Lee, H. S.; Niemeyer, M.; Törnroos, K. W.; Anwander, R. Rare-Earth Metal Bis(tetramethylaluminate) Complexes Supported by a Sterically Crowded Triazenido ligand. *Dalton Trans.* **2010,** 39, 6815-6825.

(29) Lee, W.-T.; Zeller, M.; Lugosan, A. Bis(triazenide), Tris(triazenide), and Lantern-Type of Triazenide Iron Complexes: Synthesis and Structural Characterization. *Inorg. Chim. Acta.* **2018,** 477, 109-113.

(30) Evans, W. J.; Walensky, J. R.; Ziller, J. W.; Rheingold, A. L. Insertion of Carbodiimides and Organic Azides into Actinide−Carbon Bonds. *Organometallics.* **2009,** 28, 3350-3357.

(31) Hauber, S.-O.; Niemeyer, M. Stabilization of Unsolvated Europium and Ytterbium Pentafluorophenyls by π-Bonding Encapsulation through a Sterically Crowded Triazenido Ligand. *Inorg. Chem.* **2005,** 44, 8644-8646.

(32) Hauber, S.-O.; Woo Seo, J.; Niemeyer, M. Halogenomercury Salts of Sterically Crowded Triazenides - Convenient Starting Materials for Redox-Transmetallation Reactions. *Z. Anorg. Allg. Chem.* **2010,** 636, 750-757.

(33) Turner, Z. R.; Bellabarba, R.; Tooze, R. P.; Arnold, P. L. Addition-Elimination Reactions across the M−C Bond of Metal N-Heterocyclic Carbenes. *J. Am. Chem. Soc.* **2010,** 132, 4050-4051.

(34) Foley, S. R.; Bensimon, C.; Richeson, D. S. Facile Formation of Rare Terminal Chalcogenido Germanium Complexes with Alkylamidinates as Supporting Ligands. *J. Am. Chem. Soc.* **1997,** 119, 10359-10363.

(35) Hey, E.; Ergezinger, C.; Dehnicke, K. Synthesis and Crystal-Structure of the Amidinato Complex Ph-C$(NSiMe_3)_2TeCl_3$. *Z. Naturforsch B.* **1989,** 44, 205-207.

(36) Gantzel, P.; Walsh, P. J. Synthesis and Crystal Structures of Lithium and Potassium Triazenide Complexes. *Inorg. Chem.* **1998,** 37, 3450-3451.

(37) Hinz, A.; Schulz, A.; Villinger, A.; Wolter, J.-M. Cyclo-Pnicta-triazanes: Biradicaloids or Zwitterions? *J. Am. Chem. Soc.* **2015,** 137, 3975-3980.

(38) Wiberg, N.; Karampatses, P.; Kühnel, E.; Veith, M.; Huch, V. Darstellung und Strukturen der Silyltriazene tBu_3Si-N-N-N(R)Si^tBu_3 (R = Na, H, Me, $SnMe_3$). *Z. Anorg. Allg. Chem.* **1988,** 562, 91-101.

(39) Klinkhammer, K. Dihypersilylstannylene and Dihypersilylplumbylene - Two Lewis-amphoteric Carbene Homologues. *Polyhedron.* **2002,** 21, 587-598.

(40) Wrackmeyer, B.; Stader, C.; Horchler, K. Multinuclear Magnetic Resonance Studies of Cyclic Monomeric Bis(amino)plumbylenes and Bis(amino)stannylenes and a New Type of Correlation Between ^{119}Sn and ^{207}Pb Chemical Shifts. *J.Magn. Reson.* **1989,** 83, 601-607.

(41) Jones, C.; Rose, R. P.; Stasch, A. Synthesis, Characterisation and Reactivity of Germanium(II) Amidinate and Guanidinate Complexes. *Dalton Trans.* **2008,** 2871-2878.

(42) Phomphrai, K.; Pongchan-O, C.; Thumrongpatanaraks, W.; Sangtrirutnugul, P.; Kongsaeree, P.; Pohmakotr, M. Synthesis of High-Molecular-Weight Poly(ε-caprolactone) Catalyzed by Highly Active Bis(amidinate) Tin(II) Complexes. *Dalton Trans.* **2011,** 40, 2157-2159.

(43) Stasch, A.; Forsyth, C. M.; Jones, C.; Junk, P. C. Thermally Stable Lead(II) Amidinates and Guanidinates. *New J. Chem.* **2008,** 32, 829-834.

(44) Jones, C.; Bonyhady, S. J.; Holzmann, N.; Frenking, G.; Stasch, A. Preparation, Characterization, and Theoretical Analysis of Group 14 Element(I) Dimers: A Case Study of Magnesium(I) Compounds as Reducing Agents in Inorganic Synthesis. *Inorg. Chem.* **2011,** 50, 12315-12325.

(45) Brym, M.; Francis, M. D.; Jin, G.; Jones, C.; Mills, D. P.; Stasch, A. Facile Transformations of a 1,3,5-Triphosphacyclohexadienyl Anion within the Coordination Sphere of Group 13 and 14 Elements: Synthesis of 1,3-Diphosphacyclopentadienyl Complexes and Phosphaorganometallic Cage Compounds. *Organometallics.* **2006,** 25, 4799-4807.

(46) Ahmet, I. Y.; Hill, M. S.; Raithby, P. R.; Johnson, A. L. Tin guanidinato complexes: oxidative control of Sn, SnS, SnSe and SnTe thin film deposition. *Dalton Trans.* **2018,** 47, 5031-5048.

(47) Chen, M.; Fulton, J. R.; Hitchcock, P. B.; Johnstone, N. C.; Lappert, M. F.; Protchenko, A. V. Synthesis and Theoretical Studies on Rare Three-Coordinate Lead Complexes. *Dalton Trans* **2007,** 2770-2778.

(48) Chlupaty, T.; Padelkova, Z.; Lycka, A.; Brus, J.; Ruzicka, A. Reactivity of Lithium n-Butyl Amidinates Towards Group 14 Metal(II) Chlorides Providing Series of Hetero- and Homoleptic Tetrylenes. *Dalton Trans.* **2012,** 41 (16), 5010-5019.

(49) Cole, M. L.; Davies, A. J.; Jones, C.; Junk, P. C.; Mckay, A. I.; Stasch, A. Aluminum and Indium Complexes derived from Guanidines, Triazenes, and Amidines. *Z. Anorg. Allg. Chem.* **2015,** 641, 2233-2244.

(50) Green, S. P.; Jones, C.; Lippert, K. A.; Mills, D. P.; Stasch, A. Complexes of an Anionic Gallium(I) N-Heterocyclic Carbene Analogue with Group 14 Element(II) Fragments: Synthetic, Structural and Theoretical Studies. *Inorg. Chem.* **2006,** 45, 7242-7251.

(51) Bjoergvinsson, M.; Roesky, H. W.; Pauer, F.; Stalke, D.; Sheldrick, G. M. Preparation and Structural Characterization of the Bis[bis(trimethylsilyl)amido]chalcogenides of Selenium and Tellurium. *Inorg. Chem.* **1990,** 29, 5140-5143.

(52) Allan, R. E.; Gornitzka, H.; Kärcher, J.; Paver, M. A.; Rennie, M.-A.; Russell, C. A.; Raithby, P. R.; Stalke, D.; Steiner, A.; Wright, D. S. Structure and reactivity of $[\{Te(NMe_2)_2\}_\infty]$; Application to the Preparation of Metalloorganic Tellurium(II) Compounds. *J. Chem. Soc., Dalton Trans.* **1996,** 1727-1730.

(53) Kumar, A.; Gadre, S. R.; Mohan, N.; Suresh, C. H. Lone Pairs: An Electrostatic Viewpoint. *J. Phys. Chem. A.* **2014,** 118, 526-532.

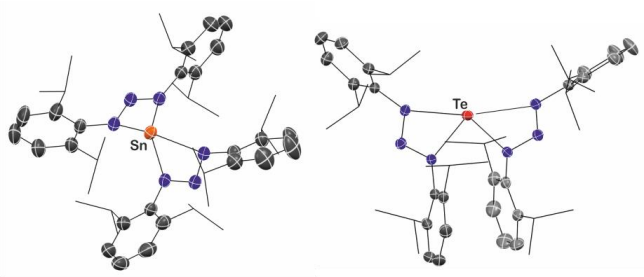

Synopsis: A series of bis-triazenide complexes of the heavier tetragen (M = Ge, Sn and Pb) and chalcogen (M = Te) elements have been synthesized by the direct reaction of the triazene with $M[N(SiMe_3)_2]_2$. These systems have been characterized by X-ray diffraction and solution NMR studies